SurfaceFlow: Large Area Haptic Display via Compliant Liquid Dielectric Actuators

Yitian Shao[1,2], Siyuan Ma[2], Sang Ho Yoon[2], Yon Visell[1] and James Holbery[2]

2020 IEEE Haptics Symposium (HAPTICS) 978-1-7281-0234-4/20/$31.00 ©2020 IEEE 10.1109/HAPTICS45997.2020.ras.HAP20.23.0f334629

***Abstract*— Touch perception is mediated by the skin, a highly compliant, distributed medium. In contrast, haptic displays frequently rely on rigid actuated elements. Here, we introduce a new haptic display based on compliant, liquid dielectric actuators. This display combines electrostatic attraction with hydraulic amplification provided by a liquid dielectric encapsulated in a compliant pouch. Voltage supplied to six pairs of opposed hydrogel electrodes generates dynamic variations in pressure on the encapsulated liquid. Mechanical amplification by the liquid enables the device to render tactile feedback with substantial displacements ($>$ 2 mm) and forces ($>$ 0.8 N) via a thin ($<$ 3.5 mm) compliant surface with a large active area (75 cm^2). The result is a soft, wearable tactile interface for providing dynamic haptic feedback to large areas of the skin. The intrinsic compliance of this interface lends a comfortable quality to the feedback it provides. We describe key considerations informing the design, including performance, reliability, and safety, and how these are addressed in our device. We describe a fabrication method that enable the device to be easily reproduced by others. We discuss a flexible multichannel system for dynamically controlling them. We also show how the display can produce unique haptic experiences, such as fluid-mediated haptic effects of motion across the skin.**

I. INTRODUCTION

Among many haptic experiences in daily life, only a few are well reproduced using existing devices [1]. One challenge is to reproduce the sensation of touching a soft, deformable object with large skin contact. A device that can provide such feedback may be useful in many applications. For example, in medical training, a haptic simulator can train physicians and improve their skill of palpation [2]. Another application is social virtual reality, allowing interpersonal touch that enhances social presence in a virtual environment [3].

It is challenging to render such experiences with conventional haptic feedback devices, many of which involve rigid elements whose attributes impair the ability of such devices to simulate many naturally soft and organic materials [4]–[6]. Recently, several skin-conformable haptic display devices based on pneumatic or hydraulic sources have been developed [7]–[11]. However, these often entail pumps that are bulky and slow to respond, making them hard to control [12]. Many haptic wearables, including gloves, integrate vibration motors. The sensations produced by such devices are rarely similar to what is felt during natural touch. There are several reasons for this, including their bandwidth limitations, which prevent them from producing controlled low frequency haptic feedback [13], [14]. While such shortcomings can be addressed via exoskeleton designs [15], such mechanical structures often further reduce the naturalness.

Material technologies for haptic feedback are rapidly advancing [12], including electrostatic actuator technologies [16]. Such actuators comprise a compliant dielectric layer sandwiched between two conductive layers. Voltage applied to the conductors produces an electric field generating charges with opposite polarities at two sides of the dielectric. Electrostatic forces act to reduce the distance between the conductive layers. In dielectric elastomer actuators (DEA), the compliance of a dielectric makes it possible for a voltage in the 10 kV range to generate small, dynamic displacements. However, such actuators have rarely been used in haptics applications, due to several commonly occurring shortcomings, including restricted dynamic range, bandwidth, and fragility. A recently proposed variation on DEAs is the hydraulically amplified electrostatic actuator [17]. These devices employ a liquid dielectric, rather than a solid, in combination with an insulating thin film layer. The liquid undergoes large bulk displacement, yielding mechanical amplification of displacement and larger forces. These devices can be driven with kV range voltages, and can be operated from batteries using suitable voltage converters [18].

Informed by these developments, we designed SurfaceFlow, a large area haptic display based on compliant, liquid dielectric actuators. This display combines electrostatic attraction with hydraulic amplification provided by a liquid dielectric encapsulated in a compliant pouch. Voltage supplied to opposed electrodes generates dynamic variations in pressure on the encapsulated liquid. The device is lightweight and thin, and could lead to skin-like body worn interfaces. The large area of contact improves mechanical transmission to the skin, and the soft rubber surface of the device lends it a comfortable feel, like skin-to-skin contact. The multiple electrostatic actuators integrated in the device enable it to provide both static and dynamic spatial patterns of tactile feedback to large areas of the skin.

The rest of the paper is organized as follows. First, we present the design and operating principles of the SurfaceFlow display device. As explained there, the design is informed by considerations of performance, reliability, and safety. We next describe how to make them using a process designed to make them easy to reproduce. We then discuss the electronic control system. We present two experiments evaluating the performance of the device, one characterizing the static and dynamic mechanical performance for both

[1] Electrical and Computer Engineering Department, University of California, Santa Barbara, CA 93106, USA yitianshao@ucsb.edu

[2] Applied Sciences Group, Microsoft Corporation, Redmond, WA 98052, USA siyma@microsoft.com

force and displacement, another assessing its effectiveness in producing tactile patterns on the hand. We conclude with a discussion of the main findings and opportunities for future research.

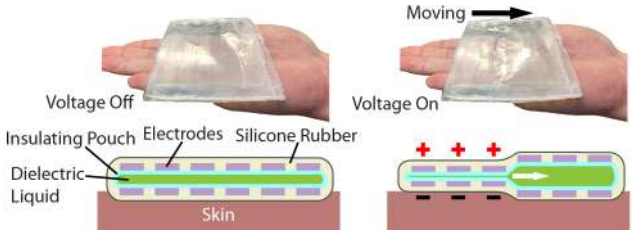

Fig. 1. Top row: Photos of the display device during operation on the hand. Bottom row: Simplified structure (cross-sectional view) and operating mechanism. The dielectric liquid is encapsulated by an insulating pouch, with opposed pairs of electrodes on each side. Voltages applied across pairs of electrodes generate electrostatic pressures that closes the gap between them, displacing the dielectric liquid to volumes between inactivated electrodes, and producing a tactile motion on the skin.

II. Design and Fabrication

A. Design and Operating Mechanism

Our device was designed to contain a liquid dielectric layer, in a thin, compliant, palm-sized pouch with six pairs of opposed electrodes. Applying a voltage to select electrode pair squeezes the liquid in the gap between them, displacing the liquid, resulting in bulk deformation of the surface (Fig. 1). The dielectric liquid is sealed inside an insulating pouch. Pairs of opposed hydrogel electrodes are affixed to the exterior of the pouch. For each pair of electrodes, one is grounded and is positioned on the side of the device facing the skin, while positive voltage is applied to the other, which is attached to the side facing away from the skin. This structure is enclosed in a silicone protective pouch, providing further protective insulation. When voltage is applied across an electrode pair, an electrostatic force is produced, compressing the dielectric liquid and causing it to be displaced to volumes between other inactivated electrodes. This causes selected regions of the device to expand, yielding force and displacement feedback that are felt by the skin. The device can be restored to its original state by applying voltage to electrodes in the expanded area.

The electrostatic force produced by each pair of electrodes depends on the applied voltage, the resulting charge between them, and the distance between electrodes [19]. Our device integrates two different dielectric materials in two layers between the electrodes. Let z_i be the total thickness of the insulating pouch layer and z_f the thickness of the dielectric liquid. Since the insulating layer undergoes little deformation, z_i is nearly a constant during actuation (for essentially any value $z_f > 0$). The electrostatic force between an opposed electrode pair is given by:

$$F = -\frac{dW}{d(z_i + z_f)} = -\frac{dW}{dz_f} \tag{1}$$

where W is the work done by closing the gap between the electrodes. The latter is given by:

$$W = \frac{1}{2} C U^2 \tag{2}$$

where U is the applied voltage. C is the total capacitance of the dielectric structure composed of the insulating layer and the dielectric liquid, with capacitances C_i and C_f respectively. Since they are connected in series:

$$\begin{aligned} &\frac{1}{C} = \frac{1}{C_i} + \frac{1}{C_f}, \\ &C_i = \frac{\varepsilon_0 \varepsilon_i A}{z_i}, \quad C_f = \frac{\varepsilon_0 \varepsilon_f A}{z_f}. \end{aligned} \tag{3}$$

Here, $\varepsilon_0 = 8.854 \times 10^{-12}$ Farad/m is the free-space permittivity. ε_i and ε_f are the relative permittivities of the insulating layer and the dielectric liquid respectively. A is the area of the electrodes. Combining equations (1), (2) and (3), we obtain:

$$F = \frac{1}{2} \varepsilon_0 \varepsilon_f A \frac{U^2}{(z_f + \frac{\varepsilon_f}{\varepsilon_i} z_i)^2} \tag{4}$$

To maximize the electrostatic force that squeezes the liquid, dielectric materials with high permittivity and modest thickness are needed. Moreover, these materials should possess sufficient dielectric strength to avoid electrical discharge. To achieve this, transformer oil (Envirotemp FR3, Cargill, Inc.), which is designed to have precisely these attributes, was selected as the dielectric liquid. The outer insulating layer was made from soft silicone rubber (Ecoflex 00-30, Smooth On Inc.). The electrodes were fabricated using UV-curable conductive hydrogel (JN0917-A, Polychem UV/EB International Corp). They are flexible and transparent. The finished device has a thickness of 3.27 mm and a weight of 34.4 grams. The active display area is 75 cm^2, enabling it to provide tactile feedback to large skin areas, such as the palm (Fig. 2A) or forearm.

B. Design for Reliability

One challenge in using electrostatic actuators is that device failure can be caused by dielectric discharge between electrodes. Choosing an appropriate thickness, z_i, for the insulating pouch layer avoids the possibility of dielectric breakdown. However, as z_i increases, higher voltages are needed in order to produce an equivalent force (equation (4)). We selected a thin insulating material, biaxially oriented polypropylene (BOPP), with < 18 μm thickness, inspired by prior research on similar actuators [18]. Although BOPP has a dielectric breakdown strength of 700 V/μm, defects can reduce the dielectric strength [20]. To further improve the robustness of the device, we designed a dual-layer structure to avoid this possibility. The resulting device structure is shown in Fig. 2B. Two BOPP sheets with 17.5 μm thickness (MSB, Impex Global Films) are combined below each electrode, including, for each pair, an inner layer enclosing the dielectric liquid on each side and an outer layer abutting each electrode. Owing to this structure, defect-related dielectric breakdown is unlikely, since this would only be possible if defects (which are rare) occur at overlapping locations of both layers. Either layer can be replaced easily should a damage occur, making the device repairable. As discussed below, our design ensures that dielectric breakdown, which

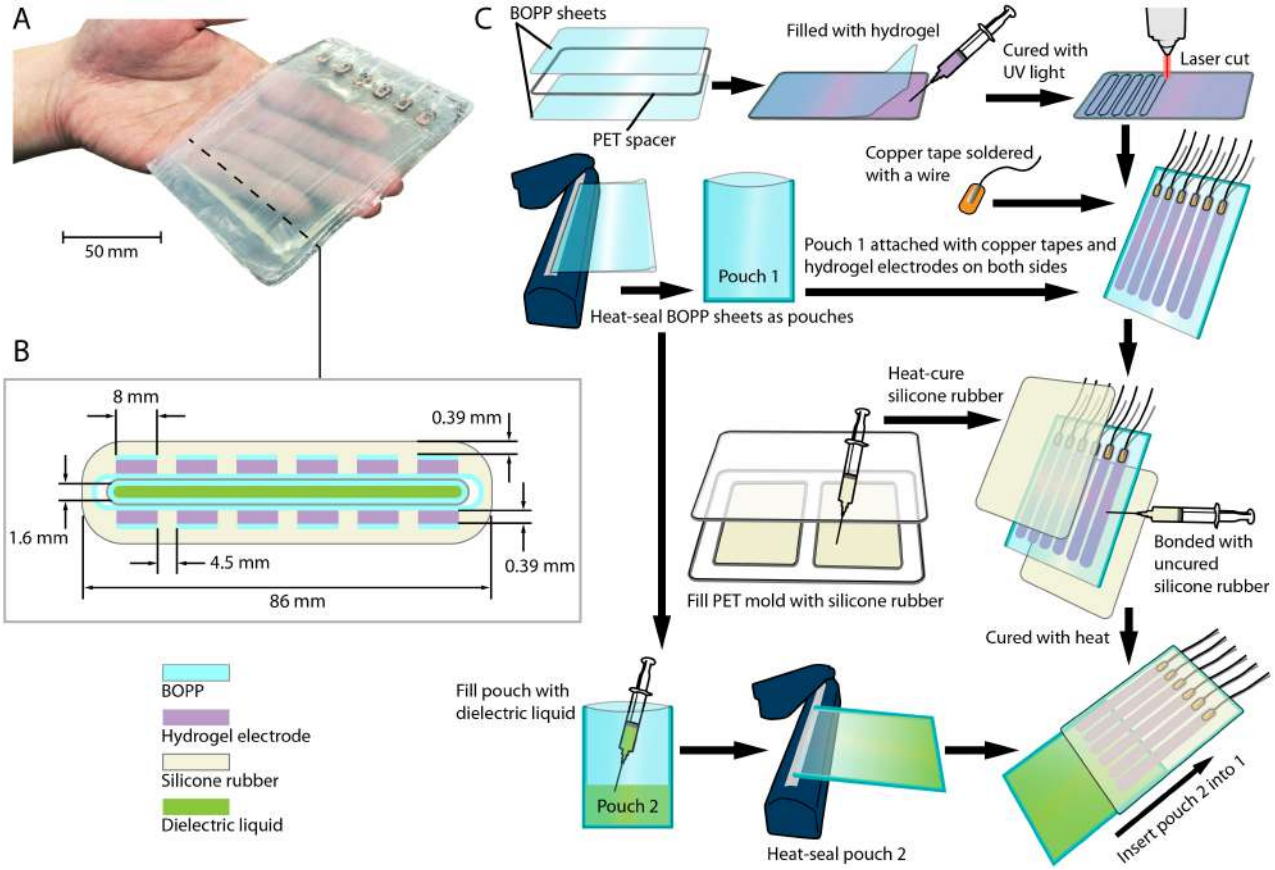

Fig. 2. A. The SurfaceFlow device is soft, flexible and translucent. B. Cross-sectional view of the device. It has two components: An inner BOPP insulating pouch layer encapsulating the dielectric liquid and an outer insulating silicone layer. Six pairs of opposed hydrogel electrodes are positioned on opposite sides of the liquid pouch. C. Overview of the fabrication procedure.

involves discharge between electrodes, poses no significant risk to a user, since charge is confined within the device.

C. Design for Safety

Electrical safety is another key consideration due to the significant operating voltages. We integrated multiple features to ensure user safety. The first is exterior electrical insulation. The entire electrostatic actuator structure is enclosed inside silicone rubber, with thickness of 390 μm and breakdown strength $>$ 13.8 V/μm. Furthermore, all electrodes are sandwiched by the BOPP sheets, providing additional electrical insulation. In addition, the device is designed to contact a user on the side in which all electrodes are connected to ground. Finally, the operating currents used by the device are low ($<$ 200 μA), poses minimal health risks to the skin [21]. This is achieved via control electronics that limit current, as discussed in section II-E.

D. Fabrication

We designed a fabrication process that would enable the device to be easily reproduced. The entire fabrication procedure is shown in Fig. 2(C). A laser cutting machine (VLS4.60, Universal Laser Systems Inc.) was used to cut materials, including BOPP and polyethylene terephthalate (PET) sheets, into desired shapes and create molds. They were cleaned with methanol and dried at room temperature. A 390 μm spacer was laser cut from PET sheet and sandwiched between two BOPP sheets. The molds were filled with 6.5 mL conductive hydrogel and cured under UV light (ECE 5000, Dymax Corporation) for 40 seconds. After this, electrodes were cut from the BOPP-shielded hydrogel. Two pouches were made from BOPP sheets with three sides heat-sealed. 50 μm copper tapes soldered with wire connections were attached to one pouch (pouch 1), and were then covered with hydrogel electrodes, forming electrical connections from the wires to the electrodes. Two 390 μm silicone rubber sheets were made by filling a PET mold with liquid silicone rubber and cured in an oven (Lab Companion Model OF-02, Jeio Tech Inc.) at 65 C$^\circ$ for 7 minutes. They were bonded to both sides of pouch 1 to cover the electrodes, using more liquid silicone rubber. After curing in the oven at 45 C$^\circ$ for 10 minutes, the electrodes were completely sealed below the silicone rubber layer. Finally, the second BOPP pouch (pouch 2) was filled with 12 mL dielectric liquid, then heat-sealed, and inserted into pouch 1.

E. Control System

A multi-channel voltage control system was developed in order to actuate each electrode pair independently (Fig. 3). The device is controlled by a PC through a data acquisition (DAQ) interface (Model 6255, National Instruments). An analog output from the DAQ is amplified to 8 kV via a power amplifier (Model 20/20 A-G, Trek, Inc.). The amplifier

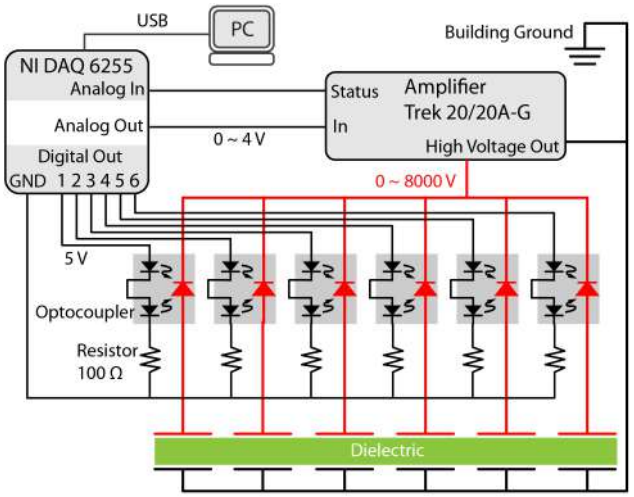

Fig. 3. Control system of the device. A PC-interfaced NI DAQ was used to control and monitor the status (output voltage and current) of the amplifier and independently regulate current in each channel using optocouplers.

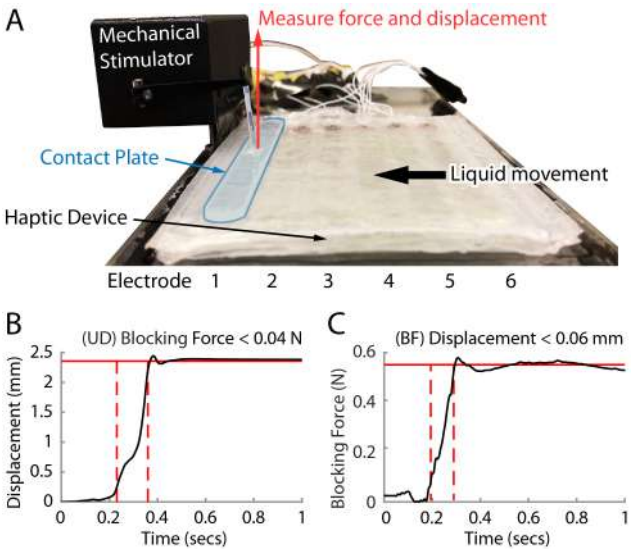

Fig. 4. Force and displacement measurement of the device using a mechanical stimulator. (A) The device was placed between the contact plate of the mechanical stimulator and a support platform. The contact plate overlapped the electrode on the left. Three pairs of electrodes on the right moved the dielectric liquid to the left, pushing the contact plate upwards against the mechanical stimulator. Example measurements: (B) Unloaded displacement (UD) of the contact plate when the mechanical stimulator outputs blocking force close to zero. (C) Blocking force (BF) of the contact plate when mechanical stimulator held the plate against the device without displacement. The solid red lines indicate time-averaged peak responses. The time duration between two dashed lines indicates the rising time.

output is distributed via switched connections to six channels connected to the electrodes of the electrostatic actuators. Each switched connection is regulated by an integrated optocoupler (OC100HG, Voltage Multipliers Inc.) that is controlled using the 5V digital output of the same DAQ. With voltage applied, the two LEDs inside the optocoupler emit light that opens the photodiode based transistor. With the 100 Ω resistor limiting the current of the LEDs, the maximum current passing through the photodiode based transistor is limited ($< 250\ \mu$A) in all high-voltage channels. Electrical current is also monitored by the PC in real time. The voltage is interrupted if the current exceeds the limit preset in the PC. These features further improve the reliability and safety of the device.

III. Validation Experiment

To evaluate the performance of the SurfaceFlow display, measurements of its force output and displacement were recorded. In addition, we evaluated the device's ability to produce tactile feedback patterns on the skin, via the palm of the hand.

A. Mechanical Evaluation

A computer-controlled mechanical stimulator (Model 300C-LR, Aurora Scientific Inc.) was used to measure the force output and displacement of the device (Fig. 4A), during actuation. An acrylic contact plate, with the same size as the first electrode of the device, was bonded to the tip of the mechanical stimulator device. The display was placed between the contact plate and a supporting platform, with the electrode on the left overlap with the contact plate. During the measurements, electrode 6, 5, and 4 were actuated consecutively from the right, displacing liquid to the left, causing electrode 1 (the leftmost) to move upward, pushing the contact plate against the mechanical stimulator. Evaluations were performed under two different measurement conditions. First, the unloaded displacement (UD) of the device was measured during maximum displacement with minimum preload (< 0.04 N). Second, blocking force (BF) of the device was measured at the maximum force that was required to prevent displacement (threshold < 0.06 mm). An example measurement in each condition is shown in Fig. 4B and C, respectively. Two features were extracted from the measurements in order to assess the performance of the device. The red solid line indicates the measurement obtained after averaging 100-millisecond measurement starting from the peak of the response curve of force (BF) or displacement (UD). This provides an estimate of the low-frequency (DC) displacements that can be produced on the skin. The two red dashed lines indicate the time instants at where the curve reached 10 % and 90 % of its peak value. The interval between them was the rise time of the response.

Measurements of the device with different actuation patterns were taken for both tests (UD and BF). For each, measurements were repeated for five times, then both the mean and standard deviation (SD) were computed. We evaluated the impact that actuation speed has on performance, by closing the three electrode pairs at different time intervals Δt (Fig. 5A). The actuation voltage was set to 8 kV. In the UD condition, the maximum displacement was 2.2 ± 0.1 mm (mean $\pm$ SD) when $\Delta t = 50$ ms, and corresponding rise time was 114 ± 17 ms, as shown in Fig. 5B. When $\Delta t = 0$, all three pairs were closed simultaneously. However, this resulted in a relatively small displacement and longer rise time, compared to asynchronous actuation, with $\Delta t = 10$, 50 or 100 ms. The device behaved very differently in the BF condition. The force output for cases with $\Delta t \leq 100$ ms were similar. The rise time of force increased with Δt.

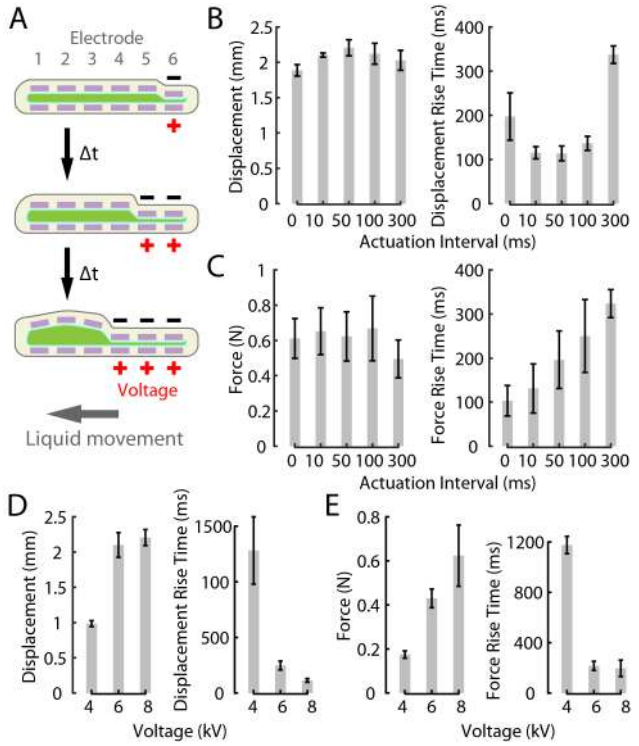

Fig. 5. Evaluation of effects of actuation speed and voltage using the configuration in Fig. 4. (A) The device was operated by closing electrode pairs consecutively with a fixed actuation interval Δt. Results: Measurements of (B) displacement (UD) and (C) force (BF) at different actuation speeds when voltage = 8 kV. Measurements of (D) displacement (UD) and (E) force (BF) with different actuation voltages when Δt = 50 ms.

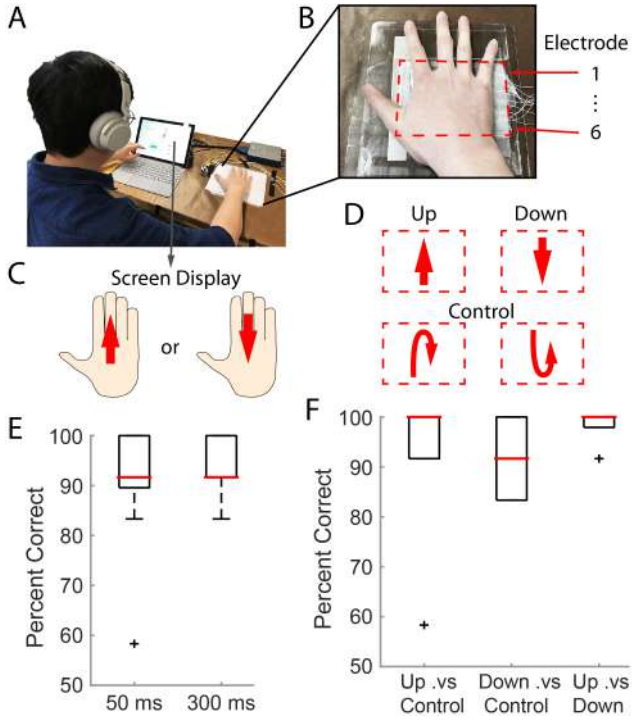

Fig. 6. User evaluation on tactile motion pattern rendering. (A) Experiment setup: Participants (B) rested their dominant hand on the device and (C) matched perceived motion with the figure displayed on the screen. (D) Two target (up and down) and two control stimuli produced in the experiment. Red arrows indicate the motion of dielectric liquid. Dashed lines illustrate the boundary of haptic display. The box plots show identification rate of target stimuli for (E) two actuation speeds and in (F) two different tasks: identifying target against control stimuli and discriminating two target stimuli.

In addition, the performance was evaluated as a function of the actuation voltage. In this case, the device was driven by 4, 6 and 8 kV, with a fixed actuation interval Δt = 50 ms. As voltage increased, both displacement (Fig. 5D) and force output (Fig. 5E) increased and rise time decreased. There were insignificant differences between displacements at 6 and 8 kV, suggesting that, by the time 50 ms had elapsed, most liquid was displaced to the space between inactive electrodes when driven with voltage $\geq$ 6 kV. However, 8 kV produced much larger force than was produced at 6 kV, as expected from the theoretical model.

B. User Study

We performed a user study to assess the device's ability to render tactile motion patterns (proximal-distal direction). Nine participants (four females and five males, aged 23 to 41 years old) volunteered to participate in the study. All participants are right hand dominant. No participants reported abnormalities affecting touch perception. The study was conducted according to both institution guidelines and national regulations on human subject research. All participants gave their informed consent. The experiment setup is shown in Fig. 6A. The participants were seated in front of a table with the device and a PC. An interface was displayed on the PC, allowing users to control the device and submit answers. In each trial, the participants rested the right palm on the display area of the device, with electrode 1 to 6 aligned from distal to proximal area of the palm (Fig. 6B). Through the user interface, participants played and experienced two stimuli, one at a time, and were asked to select the one that best matched the visual display (Fig. 6C). Participants were instructed to lift their hand after they felt a stimulus and were required to rest for 10 seconds, in order to allow the device to be fully restored to its original shape. Only one of the two stimuli produced tactile motion in the direction described by the visual display. The other one was either a control stimulus that changes direction (Fig. 6D) or a stimulus moving in the direction opposite to the visual display, yielding six combinations. In our design, only three electrodes of the device were actuated sequentially to generate a stimulus. There were two target stimuli presenting upward or downward motion (moving up by closing electrode 6, 5, 4 or down by closing 1, 2, 3) and two control stimuli (closing electrode 4, 2, 5 or 3, 5, 2). Each combination was repeated three times with actuation setting Δt = 50 ms and three times with Δt = 300 ms, as the chosen time intervals provided perceivably different tactile motion in a pilot study. Those combinations were presented in a random order, resulting in 36 trials per participant.

We logged the number of trials when participants correctly associated the stimulus they felt to the direction on the visual display. The median correct response rate was 94.4%. Mann-Whitney U tests were performed, with significance level set to p = 0.05. The effect of actuation speeds on identification

correctness (Fig. 6E) was insignificant (p = 0.61). The effect of direction of target stimuli when discriminated against control stimuli were also evaluated (Fig. 6F). The identification correctness of target stimuli moving up (median 100%) and down (median 91.7%) were similar (p = 0.37). When differentiating the two target stimuli, seven out of nine participants had 100% correctness. The results suggest that the device can produce directional tactile motions on the skin that are easily recognizable by most users. The actuation speed and direction had little effect on the performance.

IV. Conclusion and future work

We developed a large area haptic display, the SurfaceFlow, based on compliant, liquid dielectric actuators. It combines electrostatic actuation with hydraulic amplification provided by a liquid dielectric encapsulated in a compliant pouch. The device can provide dynamic tactile feedback patterns to large areas of skin.

Multiple design features ensure reliable operation, repairability and safety. We presented a fabrication method that makes the device easy to reproduce. We evaluated the performance of the device through mechanical measurements and a user study. The results demonstrate the effectiveness of the device in providing substantial and recognizable tactile feedback, including patterns of motion on the skin.

While the results are promising, several opportunities exist for extending this work. For example, while our system was operated using a lab amplifier, such a device can readily be driven by a battery and voltage converter, enabling portable use [18]. Although the voltages used can readily be provided via lab equipment or batteries, there would be advantages to enable lower operating voltages. One way to achieve this would be to employ a liquid with higher dielectric permittivity. Another would be to design a structure with multiple stacked dielectric layers. We plan to pursue both in future work. Secondly, the complex liquid dynamics can greatly affect the actuator outputs. Since electrostatic actuators have the merit of self-sensing [22], implementing a closed-loop control of the actuators could make the device output more controllable. Finally, the electrostatic actuators are capable of vibrating up to several hundred Hertz [18], covering most of the tactile sensitivity range of the human hand [23]. Such vibrations could enable richer haptic experiences to be rendered, such as contact events or textures. In future work, we will enhance the device to produce more complex tactile patterns and demonstrate its use cases, such as haptic rending of animate objects, inspired by comments in the post-experiment survey in which some participants reported a sensation of "heartbeat" or "petting a cat" after they had felt the tactile stimuli.

We envisage applications of such displays in many domains, ranging from wearable garments for social haptics to medical training interfaces and VR displays.

References

[1] H. Culbertson, S. B. Schorr, and A. M. Okamura, "Haptics: The present and future of artificial touch sensation," *Annual Review of Control, Robotics, and Autonomous Systems*, vol. 1, pp. 385–409, 2018.

[2] A. Talhan and S. Jeon, "Pneumatic actuation in haptic-enabled medical simulators: A review," *IEEE Access*, vol. 6, pp. 3184–3200, 2017.

[3] C. S. Oh, J. N. Bailenson, and G. F. Welch, "A systematic review of social presence: definition, antecedents, and implications," *Front. Robot. AI 5: 114. doi: 10.3389/frobt*, 2018.

[4] B. Son and J. Park, "Tactile sensitivity to distributed patterns in a palm," in *Proceedings of the 2018 on International Conference on Multimodal Interaction*. ACM, 2018, pp. 486–491.

[5] D. Leithinger, S. Follmer, A. Olwal, and H. Ishii, "Physical telepresence: shape capture and display for embodied, computer-mediated remote collaboration," in *Proceedings of the 27th annual ACM symposium on User interface software and technology*. ACM, 2014, pp. 461–470.

[6] J. Jiao, D. Wang, Y. Zhang, D. Cao, Y. Visell, X. Guo, and X. Sun, "Detection and discrimination thresholds for haptic gratings on electrostatic tactile displays," *IEEE transactions on haptics*, vol. 12, no. 1, pp. 34–42, 2018.

[7] A. Talhan and S. Jeon, "Programmable prostate palpation simulator using property-changing pneumatic bladder," *Computers in biology and medicine*, vol. 96, pp. 166–177, 2018.

[8] T. Taniguchi, S. Sakurai, T. Nojima, and K. Hirota, "Multi-point pressure sensation display using pneumatic actuators," in *International Conference on Human Haptic Sensing and Touch Enabled Computer Applications*. Springer, 2018, pp. 58–67.

[9] A. A. Stanley and A. M. Okamura, "Controllable surface haptics via particle jamming and pneumatics," *IEEE transactions on haptics*, vol. 8, no. 1, pp. 20–30, 2015.

[10] T. M. Simon, R. T. Smith, and B. H. Thomas, "Wearable jamming mitten for virtual environment haptics," in *Proceedings of the 2014 ACM International Symposium on Wearable Computers*. ACM, 2014, pp. 67–70.

[11] M. Zhu, T. N. Do, E. Hawkes, and Y. Visell, "Fluidic fabric muscle sheets for wearable and soft robotics," *arXiv preprint arXiv:1903.08253*, 2019.

[12] S. Biswas and Y. Visell, "Emerging material technologies for haptics," *Advanced Materials Technologies*, vol. 4, no. 4, p. 1900042, 2019.

[13] K. Tanabe, S. Takei, and H. Kajimoto, "The whole hand haptic glove using numerous linear resonant actuators," in *Proceedings of IEEE World Haptics Conference*, 2015.

[14] D. Sadihov, B. Migge, R. Gassert, and Y. Kim, "Prototype of a vr upper-limb rehabilitation system enhanced with motion-based tactile feedback," in *2013 World Haptics Conference (WHC)*. IEEE, 2013, pp. 449–454.

[15] C. Pacchierotti, S. Sinclair, M. Solazzi, A. Frisoli, V. Hayward, and D. Prattichizzo, "Wearable haptic systems for the fingertip and the hand: taxonomy, review, and perspectives," *IEEE transactions on haptics*, vol. 10, no. 4, pp. 580–600, 2017.

[16] A. O'Halloran, F. O'malley, and P. McHugh, "A review on dielectric elastomer actuators, technology, applications, and challenges," *Journal of Applied Physics*, vol. 104, no. 7, p. 9, 2008.

[17] E. Acome, S. Mitchell, T. Morrissey, M. Emmett, C. Benjamin, M. King, M. Radakovitz, and C. Keplinger, "Hydraulically amplified self-healing electrostatic actuators with muscle-like performance," *Science*, vol. 359, no. 6371, pp. 61–65, 2018.

[18] S. K. Mitchell, X. Wang, E. Acome, T. Martin, K. Ly, N. Kellaris, V. G. Venkata, and C. Keplinger, "An easy-to-implement toolkit to create versatile and high-performance hasel actuators for untethered soft robots," *Advanced Science*, p. 1900178, 2019.

[19] Z. Suo, "Theory of dielectric elastomers," *Acta Mechanica Solida Sinica*, vol. 23, no. 6, pp. 549–578, 2010.

[20] X. Liu, S. Jia, B. Li, Y. Xing, H. Chen, H. Ma, and J. Sheng, "An electromechanical model for the estimation of breakdown voltage in stretchable dielectric elastomer," *IEEE Transactions on Dielectrics and Electrical Insulation*, vol. 24, no. 5, pp. 3099–3112, 2017.

[21] K. Oldham-Smith and J. M. Madden, *Electrical Safety and the Law*. Wiley-Blackwell, 2002.

[22] K. Jung, K. J. Kim, and H. R. Choi, "A self-sensing dielectric elastomer actuator," *Sensors and Actuators A: Physical*, vol. 143, no. 2, pp. 343–351, 2008.

[23] R. S. Johansson and J. R. Flanagan, "Coding and use of tactile signals from the fingertips in object manipulation tasks," *Nature Reviews Neuroscience*, vol. 10, no. 5, p. 345, 2009.